ISSN 0023-1584, Kinetics and Catalysis, 2006, Vol. 47, No. 5, pp. 704–714. © MAIK "Nauka/Interperiodica" (Russia), 2006.
Original Russian Text © L.I. Kuznetsova, N.I. Kuznetsova, S.V. Koshcheev, V.A. Rogov, V.I. Zaikovskii, B.N. Novgorodov, L.G. Detusheva, V.A. Likholobov, D.I. Kochubey, 2006, published in Kinetika i Kataliz, 2006, Vol. 47, No. 5, pp. 728–737.

Interaction of Platinum and Molybdophosphoric Heteropoly Acid under Conditions of Catalyst Preparation for Benzene Oxidation to Phenol with an O_2–H_2 Gas Mixture

L. I. Kuznetsova[a], N. I. Kuznetsova[a], S. V. Koshcheev[a], V. A. Rogov[a], V. I. Zaikovskii[a], B. N. Novgorodov[a], L. G. Detusheva[a], V. A. Likholobov[b], and D. I. Kochubey[a]

[a] *Boreskov Institute of Catalysis, Siberian Branch, Russian Academy of Sciences, Novosibirsk, 630090 Russia*
e-mail: kuznina@catalysis.nsk.su

[b] *Institute of Hydrocarbon Processing, Siberian Branch, Russian Academy of Sciences, Omsk, 644040 Russia*

Received March 9, 2005

Abstract—The transformations of platinum and a heteropoly acid (HPA) in binary systems prepared from H_2PtCl_6 or H_2PtCl_4 and $H_3PMo_{12}O_{40}$ were studied using IR and UV–VIS spectroscopy, elemental analysis, XPS, EXAFS, TPR, and HREM. The calcination of platinum chloride with the HPA to 450°C resulted in the formation of a platinum salt of the HPA along with decomposition products (mixture **I**). The reduction of calcined samples containing Pt : HPA = 1 : 1 with hydrogen at 300°C (mixture **II**) followed by exposure to air resulted in the regeneration of the HPA structure. The resulting solid samples of $Pt^0_{1-n}Pt^{II}_n Cl_mO_xH_y) \cdot (H_{3+p}PMo^{VI}_{12-p}Mo^{V}_p O_{40})$ (**III**) contained platinum and molybdenum in both oxidized and reduced states. The following association species were isolated from mixtures **I** and **II** by dissolving in water: $[Pt^{II}_n PMo_{12}O_{40}]$ ($\mathbf{I_s}$) (n = 0.3–0.8) and $[Pt^0_nPMo^{red}_{12} O_{40}]$ ($\mathbf{II}_s$) ($n \approx 1$). Under exposure to air, the solutions of $\mathbf{I}_s$ were stable (pH ~2), whereas Pt^{met} was released from $\mathbf{II}_s$. After the drying of $\mathbf{I}_s$, the solid association species $(Pt^{II}_n Cl_mO_xH_y) \cdot (H_3PMo_{12}O_{40})$, where n = 0.3–0.8, m = 0.2–1, and x = 3–0, ($\mathbf{I}_{solid}$) were obtained. The $\mathbf{I}_{solid}/SiO_2$ supported samples were prepared by impregnating SiO_2 with a solution of $\mathbf{I}_s$ and drying at 100°C. Platinum metal particles of size ~20 Å and a mixed-valence association species of platinum with the HPA were observed after the reduction of $\mathbf{I}_{solid}/SiO_2$ with hydrogen at 100–250°C. These samples were active in the gas-phase oxidation of benzene to phenol at 180°C with the use of an O_2–H_2–N_2 mixture.

DOI: 10.1134/S0023158406050089

INTRODUCTION

Previously, we studied the catalytic properties of systems based on platinum group metals and heteropoly compounds in liquid-phase hydrocarbon oxidation with a gas mixture of oxygen and hydrogen. Various combinations of platinum group metals and heteropoly compounds were used: (1) solutions or supported Pd(II) or Pt(II) complexes with heteropolytungstates [1, 2], (2) solutions of heteropoly acids or their salts and a platinum group metal supported on SiO_2 or carbon [3, 4], and (3) a solid catalyst prepared from the complex salt $[Pt(NH_3)_4][H_2PMo_{12}O_{40}]_2 \cdot 7H_2O$ [5]. A supported catalyst for the gas-phase hydroxylation of benzene with an O_2–H_2 mixture was prepared with the use of platinum chloride and molybdophosphoric heteropoly acid (HPA) as precursors [6, 7]. A necessary condition for the catalytic activity of all of the systems examined is the contact of a platinum group metal with the second component (heteropoly compound) [2, 5]. The nature of the interaction between a platinum group metal and the heteropoly compound can differ depending on the composition of the parent compounds and catalyst preparation procedures [8].

In this work, we studied the interaction of platinum and the HPA in binary systems prepared from H_2PtCl_6 (or H_2PtCl_4) and $H_3PMo_{12}O_{40}$ under conditions of the preparation of a SiO_2-supported catalyst for the gas-phase oxidation of benzene with the use of an O_2–H_2–N_2 mixture. Both platinum chlorides and the HPA interact weakly with SiO_2 [9]. For this reason, their transformations were studied in the absence of SiO_2 in order to obtain the most reliable data on the nature of the interaction of platinum and the HPA. The states of platinum and the HPA were monitored at various stages of treatment: the preparation of an aqueous solution of H_2PtCl_6 (or H_2PtCl_4) and $H_3PMo_{12}O_{40}$, the drying of the solution and the calcination of the mixture, reduction in flowing H_2, and storage in air.

EXPERIMENTAL

Preparation of Pt-HPA samples. The Pt-HPA samples were prepared by mixing the aqueous solutions of H_2PtCl_6 (or H_2PtCl_4) and $H_3PMo_{12}O_{40}$ at various Pt : HPA molar ratios (from 1 to 0.1). The dry samples obtained after the evaporation of water were dried more thoroughly at 100°C, calcined in air at 300–450°C, and reduced in flowing H_2 at 300°C for 1.5 h. Before measurements, the reduced samples were usually kept in air for a day.

To prepare a supported sample, silica gel (S_{sp} = 270 m^2/g; V_{pore} = 0.8 cm^3/g; granules of 0.2–0.5 mm) was impregnated with a solution of $Pt_{0.66} \cdot H_3PMo_{12}O_{40}$ (20 wt % HPA and 1.4 wt % Pt) and dried in air and then at 100°C.

Chemical analysis of Pt-HPA samples. The concentrations of Pt, P, and Mo were determined by atomic absorption spectrometry.

IR spectroscopy. The IR spectra of Pt-HPA samples were recorded on a Specord IR-75 instrument ~1 h, one day, or a few days after calcination or reduction procedures; a sample of 3 mg in 500 mg of KBr was used.

Electronic absorption spectroscopy. The electronic absorption spectra of solutions in the visible region were measured on a Specord M-40 instrument using glass cells; water was used as a reference solution.

X-ray photoelectron spectroscopy (XPS). XPS spectra were recorded on a VG ESCALAB HP instrument. The samples were fixed on a holder using a conducting double-sided adhesive tape. The spectra were measured in a vacuum at room temperature with the excitation of photoelectrons by AlK_α radiation ($h\nu$ = 1486.6 eV) from an anticathode filtered with an Al window. The atomic ratios of elements in the sample were calculated using tabulated empirical atomic sensitivity factors [10] after the XPS measurements of narrow regions of the core levels of corresponding atoms. The scale of binding energies was precalibrated using gold, silver, and copper foils with reference to the Au4$f_{7/2}$ (84.0 eV), Ag3$d_{5/2}$ (368.3 eV), and Cu2$p_{3/2}$ (932.7 eV) lines, respectively. The binding energies of peaks were corrected for sample charging using the C1s line (284.8 eV) for bulk Pt-HPA samples and the Si2p line (103.4 eV) for SiO_2-supported samples. The accuracy of the determination of binding energies for these samples was ±0.2 eV. The line shape analysis was performed using the CALS program, which allowed us to reduce the spectra to a zero background using the Shirley method [11] after preliminary Fourier treatment and to approximate the shape of a complex multicomponent peak or doublet. The approximating doublet for an individual component with splitting parameters and a peak ratio was used in the deconvolution of Pt and Mo spectra. Individual peaks were approximated by the sum of mixed Gaussian and Lorentzian individual components [11].

Temperature-programmed reduction (TPR) with hydrogen. The TPR with hydrogen was performed using a flow system with a thermal-conductivity detector. Before the reduction, the sample was treated in O_2 for 0.5 h at 300°C, cooled to room temperature in O_2, and purged with argon. The sample weight was 100–200 mg; the flow rate of a reducing mixture (10% H_2 in Ar) was 40 cm^3/min; the heating rate was 10 K/min.

High-resolution electron microscopy (HREM). The high-resolution transmission electron microscopic images were obtained on a JEM-2010 instrument with a maximum grid resolution of 0.14 nm and an accelerating voltage of 200 kV. The samples were prepared from a powder suspension in hexane by deposition onto a porous carbon material fixed on copper gauze.

EXAFS spectroscopy. The platinum L_3-edge EXAFS spectra were measured at the EXAFS Station of the Siberian Synchrotron Radiation Center at an electron energy of 2 GeV in the VEPP-3 storage ring and a current of 90 mA in a transmission mode. The spectrometer had a channel-cut double-crystal Si(111) monochromator and proportional chambers as detectors. The data were processed according to a standard procedure with the use of the VIPER program [12] for the separation of the oscillating part of the absorption coefficient and the EXCURV-92 program [13] for the simulation of structural data. The spectra were simulated in the wavenumber range 3.5–14 $Å^{-1}$ for data as $k^3\chi(k)$.

Catalytic measurements. The catalytic measurements were performed in a flow reactor with the inner circulation of a gas phase (a so-called Berty reactor). The inlet O_2, H_2, and N_2 flow rates were specified using mass flow controllers; benzene was supplied using a syringe-type pump. The gas flow rates were 10, 5, 8, and 85 ml/min for H_2, O_2, C_6H_6, and N_2, respectively. The reaction temperature was 180°C; the catalyst weight was 0.3 g. The unit was equipped with a system for the GC analysis of gases at the reactor outlet.

RESULTS AND DISCUSSION

In the initial solutions, platinum chlorides did not react with $H_3PMo_{12}O_{40}$, as evidenced by the additivity of absorption spectra measured in the visible region for the mixtures of H_2PtCl_6 (or H_2PtCl_4) and the HPA at [H_2PtCl_6] (or H_2PtCl_4) = [$H_3PMo_{12}O_{40}$] = 0.025 mol/l at pH 1 (or pH 0.8 for H_2PtCl_4). Figure 1 shows corresponding spectra for the solutions of H_2PtCl_6 and the HPA.

In the dried samples of platinum chloride and the HPA after calcination (samples **I**) and after the subsequent reduction with hydrogen (samples **II**) followed by keeping in air (sample **III**, see scheme), the state of the HPA was monitored using IR spectra. At a molar ratio of H_2PtCl_4 : $H_3PMo_{12}O_{40}$ = 1, the calcination temperature of samples **I** was varied. After heating at 300

Chemical transformations in a two-component system of H_2PtCl_6 (or H_2PtCl_4) and $H_3PMo_{12}O_{40}$

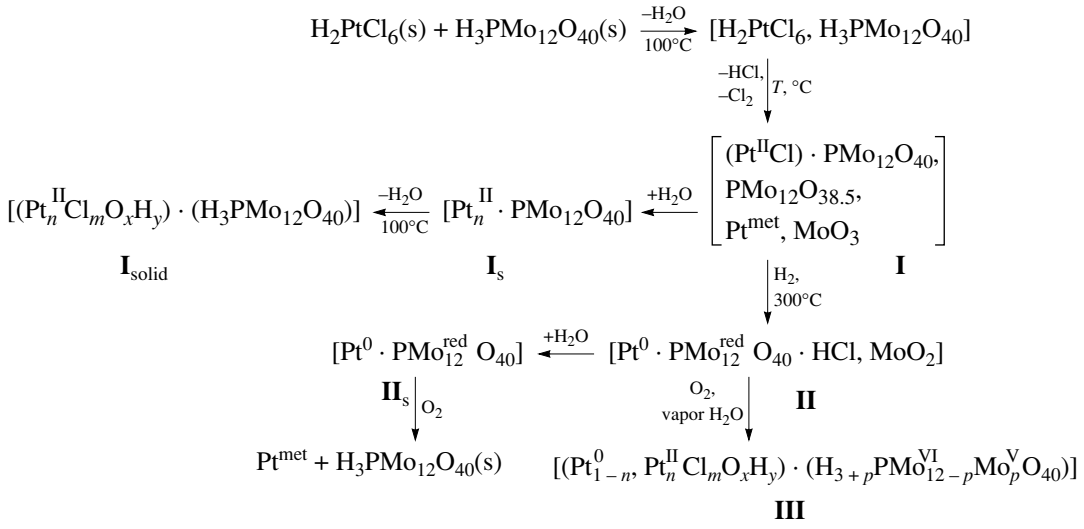

Scheme.

or 385°C, the Keggin structure of the HPA was completely retained, as evidenced by the absorption bands of the heteropoly anion at 1060 (PO_4), 960 (Mo=O), 860, and 780 cm^{-1} (Mo–O_b–Mo and Mo–O_c–Mo, respectively) (Fig. 2, spectrum *1*). After heating at 450°C, the IR spectrum of the HPA changed. Depending on the heating regime, the positions and intensities of absorption bands due to Mo–O–Mo bridging atoms at 890–795 cm^{-1} changed (Fig. 2, spectrum *2*) likely because of the formation of a Pt salt of the HPA, or deeper changes occurred in the spectrum (Fig. 2, spectrum *3*), which were related to the conversion of the HPA into the anhydride $PMo_{12}O_{38.5}$ and, partially, MoO_3 [14, 15]. Upon calcination, a small portion of platinum was deposited as a metallic mirror on the walls of the porcelain crucible. The same changes in the spectra of the HPA occurred upon the heating of a mixture of H_2PtCl_6 with $H_3PMo_{12}O_{40}$.

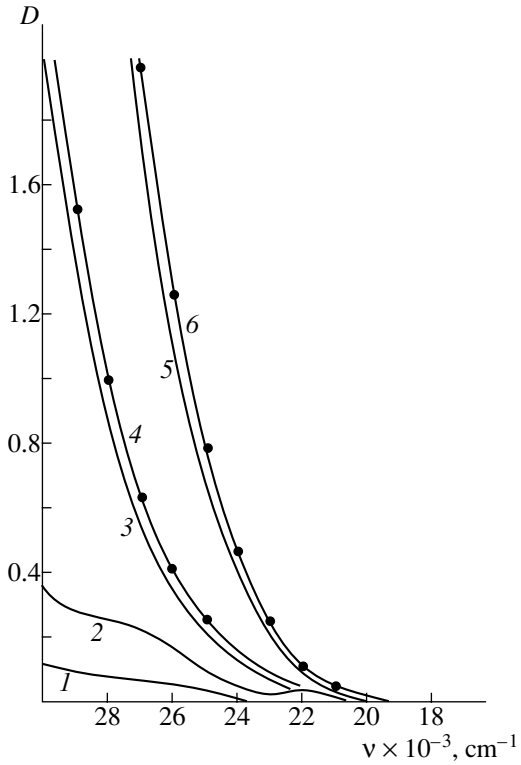

Fig. 1. Absorption spectra of H_2PtCl_6 and $H_3PMo_{12}O_{40}$ solutions and their mixture: (*1*, *2*) $[H_2PtCl_6] = 0.025$ mol/l; (*3*, *5*) $[H_3PMo_{12}O_{40}] = 0.025$ mol/l, pH 1; (*4*, *6*) $[H_2PtCl_6] = [H_3PMo_{12}O_{40}] = 0.025$ mol/l, pH 1; points indicate the sum of the absorption of H_2PtCl_6 and $H_3PMo_{12}O_{40}$ solutions. Cell: *l* = (*1*, *3*, *4*) 0.06 or (*2*, *5*, *6*) 0.207 mm.

The keeping of samples **I** in air from 1 h to a few days after calcination did not cause changes in the IR spectra. The reduction of **I** in a flow of H_2 at 300°C followed by keeping in air for about a day caused HPA structure regeneration in sample **III** (Fig. 2, spectrum *4*).

The IR spectra of samples **II** measured ~1 h after the reduction of **I** with hydrogen (Fig. 3) suggest the interaction of platinum with the heteropoly anion. Specifically, the stability of the anion under reduction conditions depends on the ratio $H_2PtCl_4 : H_3PMo_{12}O_{40}$. After the reduction of a sample with $H_2PtCl_4 : H_3PMo_{12}O_{40} = 1$, which was preheated at 450°C, the IR spectrum exhibited absorption bands due to the heteropoly anion at 1050, 955, 850, and 780 cm^{-1} (Fig. 3, spectrum *1*). The structure of the heteropoly anion was distorted upon reduction to a greater extent at a low platinum content ($H_2PtCl_6 : H_3PMo_{12}O_{40} = 0.1$), as judged from the broadening of an absorption band at 1050 cm^{-1} due to the PO_4 tetrahedron and changes in the spectrum in the region of Mo–O–Mo bridging atom vibrations (Fig. 3,

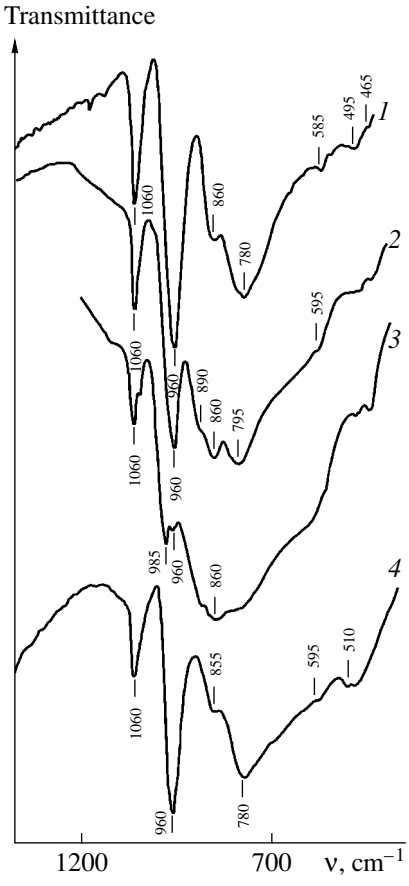

Fig. 2. IR spectra of the samples of **I** prepared from H_2PtCl_4 and $H_3PMo_{12}O_{40}$ (1 : 1, mole fraction) (*1–3*) after thermal treatment and (*4*) after the subsequent reductive treatment and keeping in air for about a day (sample **III**): $T_{calcination}$ = (*1*) 385, (*2*, *3*) 450 (measured ~1 h after calcination), or (*4*) 450°C.

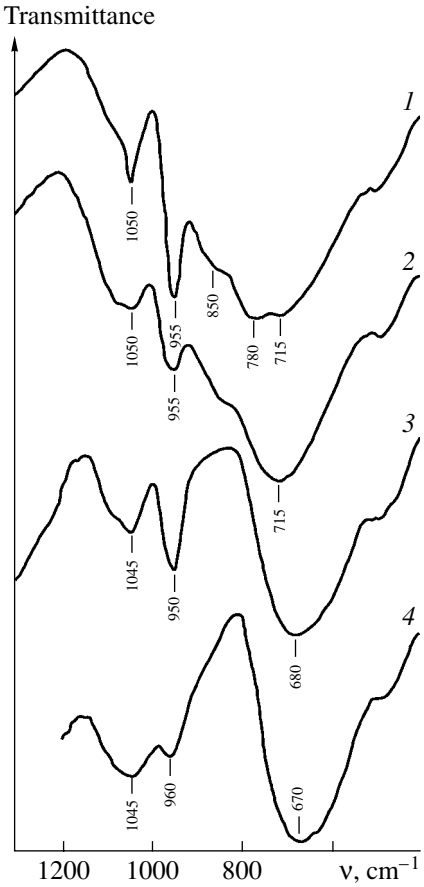

Fig. 3. IR spectra of the samples of **II** prepared from (*1*, *3*, *4*) H_2PtCl_4 and $H_3PMo_{12}O_{40}$ (1 : 1, mole fraction) or (*2*) H_2PtCl_6 and $H_3PMo_{12}O_{40}$ (0.1 : 1, mole fraction) calcined at various temperatures and reduced with hydrogen (measured ~1 h after reduction): $T_{calcination}$ = (*1*, *2*) 450, (*3*) 385, or (*4*) 300°C.

spectrum *2*). It is likely that platinum reacted with the HPA to a smaller extent if the samples with H_2PtCl_4 : $H_3PMo_{12}O_{40}$ = 1 were heated at a lower temperature of 385 or 300°C. Profound changes in the spectrum were also observed upon the reduction of these samples with hydrogen: a broadening of an absorption band at 1050 cm^{-1}, the disappearance of an absorption band at 850 cm^{-1}, and a decrease in the absorption band intensity at 960 cm^{-1} (Fig. 3, spectra *3*, *4*). These changes were attributed [16] to the degradation of the heteropoly anion structure due to deep reduction.

The mutual effect of platinum and the HPA was observed in water-soluble binary association species $\mathbf{I}_s$ (prepared from samples **I**) and $\mathbf{II}_s$ (prepared from sample **II**) (see the scheme). To prepare $\mathbf{I}_s$ and $\mathbf{II}_s$, weighed portions (~0.2 g) of samples **I** or **II** were mixed with 10 ml of water and kept for a day (or ~3 h in the case of reduced sample **II**). The undissolved portion (Pt metal and MoO_3) was filtered off, and the solutions were analyzed for Pt, P, and Mo concentrations.

The compounds isolated were found to have the composition $[Pt_n \cdot PMo_{12}]$ ($n \approx 0.3$–0.8) ($\mathbf{I}_s$) (Table 1, nos. 1–4) when obtained from mixture **I** (see the scheme), which could be prepared from either Pt(II) or Pt(IV). After the reduction of **I** in a flow of hydrogen, the composition of soluble compounds (scheme) corresponded to the formula $[Pt_n \cdot PMo_{12}]$ ($n \approx 1$) ($\mathbf{II}_s$) (Table 1, no. 5). In a further XPS study of $\mathbf{I}_s$ and $\mathbf{II}_s$, a small amount of Cl^- ions was detected in these samples.

According to elemental analysis data, the atomic ratio n = Pt : P in samples $\mathbf{I}_s$ increased with calcination temperature in the range 300–450°C (Table 1, nos. 1–3). In the above samples, the yield of PMo_{12} (based on the initial amount) somewhat decreased after calcination at 450°C because of the formation of MoO_3. The reduced sample **II** was almost completely soluble in water. The solutions of $\mathbf{I}_s$ with pH ~2 remained stable on long storage (for several months), whereas the solutions of $\mathbf{II}_s$ were unstable: platinum metal was formed upon keep-

Table 1. Composition of water-dissolved compounds obtained after the stage of calcination (nos. 1–4) and the subsequent stage of reduction (no. 5) of H_2PtCl_4 (or H_2PtCl_6) and $H_3PMo_{12}O_{40}$ samples, their yields (calculated on a molybdenum basis with reference to the initial amount in the sample), and pH of solutions

Sample	Initial composition	T, °C	P : Mo : Pt (atomic)	Yield, % (on a Mo basis)	pH
1 ($\mathbf{I}_s$)	Pt(II) : HPA = 1	300	1 : 11.4 : 0.31	76	1.6
2 ($\mathbf{I}_s$)	The same	385	1 : 11.4 : 0.43	77	1.7
3 ($\mathbf{I}_s$)	The same	450	1 : 11.7 : 0.81	60	1.8
4 ($\mathbf{I}_s$)	Pt(IV) : HPA = 0.75	450	1 : 12.6 : 0.56	63	1.8
5 ($\mathbf{II}_s$)	Pt(IV) : HPA = 1	450	1 : 12.3 : ~1 1 : 12.3 : 0.04*	100	1.8

* After the precipitation of platinum metal from solution.

ing in air, whereas $H_3PMo_{12}O_{40}$ remained in solution (Table 1, no. 5).

The electronic absorption spectra in the visible region allowed us to characterize the state of platinum and the HPA in the solutions of $\mathbf{I}_s$ and $\mathbf{II}_s$. The intensity of the absorption spectra of solutions of $\mathbf{I}_s$ increased with the calcination temperature of samples from which they were prepared over the range 300–450°C (Fig. 4, spectra *1*–*3*). The samples prepared from H_2PtCl_4 and H_2PtCl_6 and calcined at 450°C exhibited similar absorption spectra upon dissolution (Fig. 4, spectra *3*, *4*). These spectra contained strong charge-transfer bands at 24000 ($\varepsilon \sim 10^4$) and 18000 cm^{-1} ($\varepsilon \sim 5 \times 10^3$), which were related to the presence of platinum(II) because $H_3PMo_{12}O_{40}$ exhibits only weak absorption in this spectral region (cf. Fig. 1). The reduced forms of the HPA $H_3PMo_{12}O_{40}$ (so-called heteropoly blues) exhibit intense absorption in the red region of the spectrum [17], which was attributed to the low-energy electron transfer Mo(V) ⟶ Mo(VI),

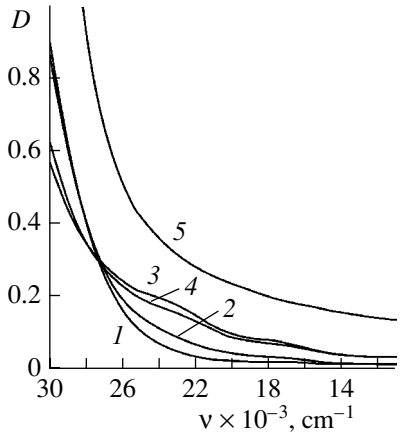

Fig. 4. Electronic absorption spectra of platinum compounds $\mathbf{I}_s$ and $\mathbf{II}_s$ with the HPA (spectra numbers correspond to sample numbers in Table 1): l = (*1*, *2*) 0.1 or (*3*–*5*) 0.06 mm; $[PMo_{12}] \approx 0.005$ mol/l; reference solution, water.

which is characteristic of mixed-valence heteropoly anions [18]. Judging from the absence of intense absorption at $\nu < 17000$ cm^{-1}, the HPA occurred in an oxidized state in the samples of $\mathbf{I}_s$.

The solution of $\mathbf{II}_s$ was characterized by intense absorption over the entire visible region. This absorption can be due to both reduced molybdenum and colloidal particles of Pt(0). The formation of the colloidal solutions of platinum group metals in the presence of polyoxometalates is well known [19, 20]. Thus, in the solutions obtained in this study, Pt(II) and Pt(0) were stabilized as the association species $[Pt_n^{II} \cdot PMo_{12}O_{40}]$ ($\mathbf{I}_s$) and $[Pt_n^0 PMo_{12}^{red} O_{40}]$ ($\mathbf{II}_s$) with molybdophosphoric heteropoly anions.

The retention of the HPA structure in Pt association species was supported using IR spectroscopy in samples $\mathbf{I}_{solid}$, which were prepared by the evaporation of $\mathbf{I}_s$ and drying at 100°C. The composition of platinum and HPA association species was refined, and the charge states of the elements were determined using XPS in the samples of $\mathbf{I}_{solid}$ and **III**.

Based on the calculation of the integrated intensities of XPS peaks [10], we determined the atomic ratio of the elements in samples $\mathbf{I}_{solid}$ and in sample **III**, which was reduced and kept in air for a day (scheme). The observed ratio O : Mo ≥ 40 : 12 (Table 2) corresponds to the anion $PMo_{12}O_{40}^{3-}$ plus oxygen, which can be the constituent of several crystal water molecules or bound to oxidized platinum. The atomic ratio Mo : Pt calculated from XPS spectra (Table 2, nos. 2–4) for the solid samples $\mathbf{I}_{solid}$ is close to this ratio determined from elemental analysis data for the solutions of $\mathbf{I}_s$ from which the samples were prepared (Table 1, nos. 2–4). This suggests the homogeneity of samples $\mathbf{I}_{solid}$ unlike the sample **III**. In the latter case, the Pt content found using XPS was higher than that taken for the synthesis by a factor of 2 (Table 2, no. 5); this can be due to the localization of reduced platinum particles on the surface of small sample particles. Chlorine was present in the test

samples. The atomic ratio of chlorine to platinum decreased in samples $\mathbf{I}_{solid}$ as the calcination temperature of precursors was increased; it was Pt : Cl < 1 after calcination at 450°C (Table 2, nos. 2–4). Sample **III** also contained a small amount of chlorine (Table 2, no. 5).

In the XPS spectra of samples $\mathbf{I}_{solid}$, the binding energy of Pt4$f_{7/2}$ was equal to 73.8 eV (Fig. 5a, spectra *2–4*), which corresponds to the Pt(II) state. In the sample of **III** reduced and kept in air for a day (Fig. 5b), a weaker doublet at 73.8 eV belonged to Pt(II), whereas most of the platinum was in the state with the Pt4$f_{7/2}$ binding energy of 72.4 eV. Based on the binding energy of 72.4 eV, this new peak occupies an intermediate position between platinum metal (71.2 eV) and chloride or oxygen compounds of Pt(II) [10]. This peak may be attributed to reduced platinum particles stabilized by the HPA.

In samples $\mathbf{I}_{solid}$, the Mo3$d_{5/2}$ binding energy was equal to 233.6 eV (Fig. 5c, spectra *2–4*). In sample **III**, a portion of molybdenum (~20%) was in the state with the Mo3$d_{5/2}$ binding energy equal to 232.3 eV (Fig. 5d, spectrum *5*). Taking into account the retention of the PMo_{12} structure in samples $\mathbf{I}_{solid}$ and **III** based on IR-

Table 2. Atomic ratios between the elements according to XPS data in dried water-soluble fractions (nos. 2–4) and a reduced sample (no. 5), which were prepared at various calcination temperatures of mixtures with (nos. 2, 3) $H_2PtCl_4 : H_3PMo_{12}O_{40}$ = 1 and $H_2PtCl_6 : H_3PMo_{12}O_{40}$ = (no. 4) 0.75 or (no. 5) 1

Sample	*T*, °C	Mo : O : Pt : Cl			
2 ($\mathbf{I}_{solid}$)	385	12	41	0.67	1.0
3 ($\mathbf{I}_{solid}$)	450	12	42	0.77	0.58
4 ($\mathbf{I}_{solid}$)	450	12	43	0.34	0.22
5 (**III**)	450	12	40	2.1	0.40

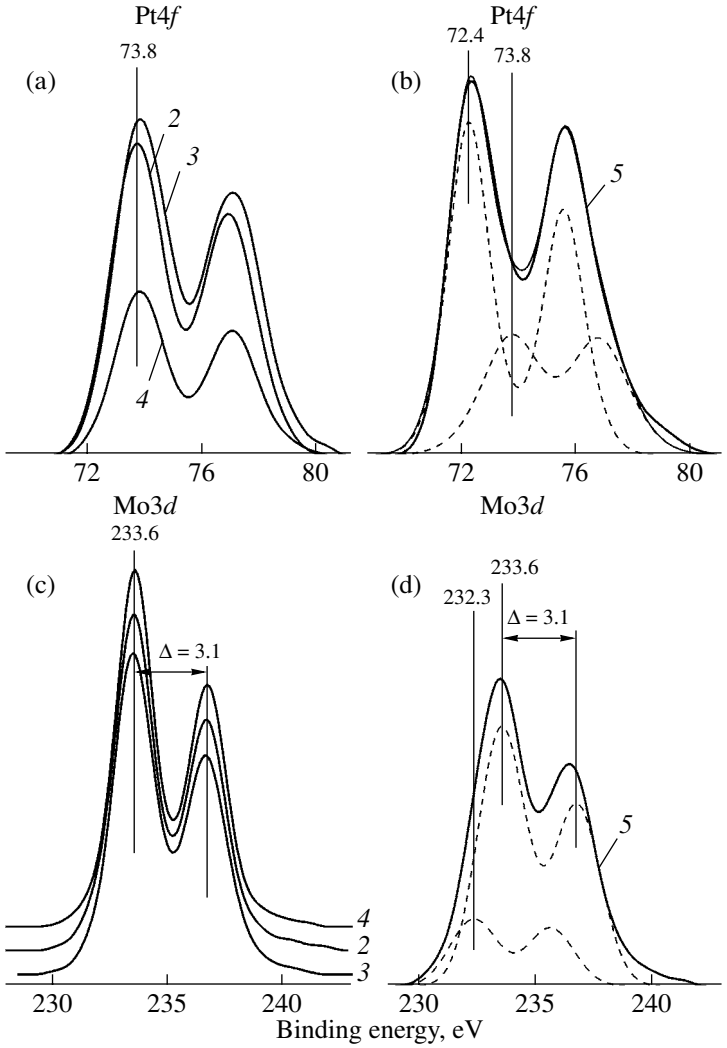

Fig. 5. XPS spectra of the samples of (*2–4*) $\mathbf{I}_{solid}$ and (*5*) **III** a day after reduction (sample numbers are specified in Table 2).

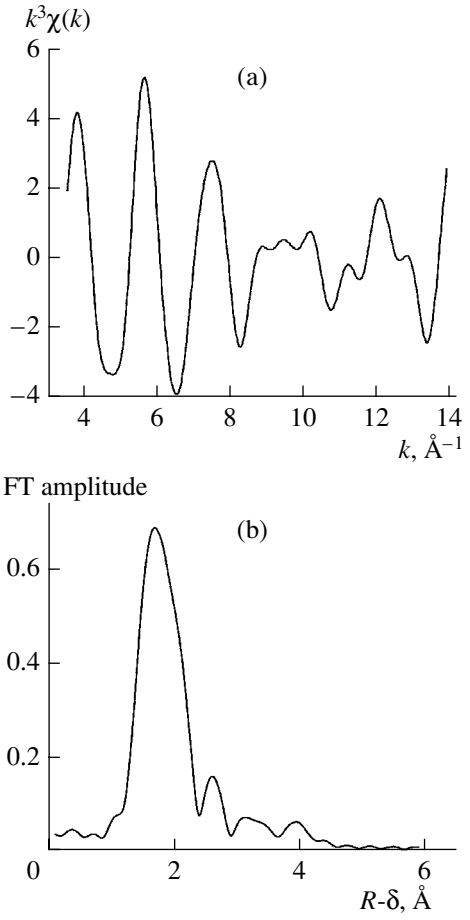

Fig. 6. (a) Initial EXAFS spectrum as $k^3\chi(k)$ of compound $\mathbf{I}_{solid}$ (obtained at $[H_2PtCl_6] = [H_3PMo_{12}O_{40}] = 1$; $T_{calcination}$ = 450°C); (b) Fourier transform amplitude.

spectroscopic data, we attributed the peak at 233.6 eV to Mo(VI) and the peak at 232.3 eV to Mo(V) as a constituent of the HPA. The assignment of Mo3*d* XPS doublets is based on a consideration of the character of electron localization in reduced Keggin structure heteropolymolybdates. Electrons additionally introduced in the course of reduction are localized at single molybdenum atoms rather than having a common molecular orbital that covers the entire heteropoly anion. An analysis of the ESR spectra of Mo(V) suggests that the electrons introduced in during reduction undergo thermally induced (jumpwise) delocalization within one heteropoly anion $PMo_{12}O_{40}^{n-}$ [17, 21]. Because the characteristic time of photoelectron emission is shorter than the electron residence time on a molybdenum atom, the individual doublets observed for sample **III** can be due to Mo(VI) and Mo(V) ions within the same heteropoly anion. A comparison of the positions and intensity ratios of these components with published data [22, 23] indicated that the sample of **III** contained the two-electron blue $H_5PMo_{10}^{VI}Mo_2^{V}O_{40}$ during the measurements.

In $\mathbf{I}_{solid}$, the Cl2*p* binding energy is equal to 200.5 eV, whereas it is 199.6 eV in the sample of **III** against 198.8 eV for K_2PtCl_4 [10]. The higher binding energy is indicative of a decrease in electron density on chlorine atoms in $\mathbf{I}_{solid}$ (as well as **III**), which can result from the formation of hydroxochloride complexes of Pt(II).

The elemental and spectroscopic analysis of unreduced and reduced samples gave the following compositions: $(Pt_n^{II}Cl_mO_xH_y) \cdot (H_3PMo_{12}O_{40})$ ($\mathbf{I}_{solid}$) with the average values of n = 0.3–0.8, m = 0.2–1, and x = 0–3 and $(Pt_{1-n}^{0}Pt_n^{II}Cl_mO_xH_y) \cdot (H_{3+p}PMo_{12-p}^{VI}Mo_p^{V}O_{40})$ (**III**). Thus, in the test association species, platinum and molybdenum can change their oxidation states depending on redox treatments.

EXAFS spectroscopy was used in order to obtain information on the coordination environment of platinum in the presence of the HPA in $\mathbf{I}_{solid}$ and **III**. Figure 6 shows (a) the initial EXAFS spectrum as $k^3\chi(k)$ and (b) the Fourier transform amplitude for $\mathbf{I}_{solid}$. Analogous data were obtained for **III**. In $\mathbf{I}_{solid}$, peaks at 2 and 2.3 Å in a ratio of 3 : 1 in the radial distribution curve (Fig. 6b), which are characteristic of a square-planar environment of platinum, correspond to oxygen and chlorine atoms in the first coordination sphere of platinum. A small portion of platinum in the sample occurred as a metal, as evidenced by the Pt–Pt distance of about 2.8 Å with an effective coordination number of 0.7. The Pt–Pt distances in the range 3.00–3.15 Å, which are characteristic of oxide structures, were not observed. The spectrum contained peaks corresponding to Pt–heavy atom (Pt or Mo) distances in the region 3.5–4.3 Å; however, their small amplitudes did not allow us to perform reliable identification. In the spectrum of **III** reduced and kept in air, all of the distances characteristic of the face-centered cubic lattice of bulk platinum were present. However, coordination numbers were ~40% lower; this fact is indicative of a small particle size (about 25 Å). The presence of a small peak corresponding to a Pt–O distance of about 2 Å in the radial distribution curve suggests the presence of a fraction of oxidized platinum (no more than 20%). These are consistent with the XPS determination of the charge state of platinum on the surface of samples. Judging from the character of the Pt–O, Pt–Cl, and Pt–Pt bonds, the hydroxo complexes of Pt(II) [24] stabilized by heteropoly anions [20] were present in compound $\mathbf{I}_{solid}$. In this case, stabilization can be due to the electrostatic interaction of $(Pt_n^{II}Cl_mO_xH_y)$ particles and the heteropoly anion or the formation of hydrogen bonds between them. In the solid samples **III**, the fine particles of reduced platinum can be stabilized because of adsorption on the heteropoly anion surface.

Thus, the transformations of the chloride complexes of Pt(II) or Pt(IV) and the HPA $H_3PMo_{12}O_{40}$, which are shown in the scheme, occur in the following manner: The heating of samples to 450°C at the stage of forma-

tion of **I** is required for the removal of most of the Cl^- ions, which hinder the interaction of platinum with the HPA. Calcination is accompanied by the reduction of Pt(IV) to Pt(II) and, partially, Pt^{met} by chloride ions. Most of the platinum remains as the salt of Pt(II) with heteropoly anions. The HPA unbound to Pt(II) passes into the anhydride $PMo_{12}O_{38.5}$ and, partially, MoO_3 at 450°C. The solid hydroxo complexes of platinum stabilized by $H_3PMo_{12}O_{40}$ (compounds $\mathbf{I}_{solid}$) were prepared through the stage of separation from mixture **I** of water-soluble samples $\mathbf{I}_s$. The action of hydrogen on compounds **I** results in mixture **II**, which includes Pt^0 and reduced heteropoly anions and, possibly, their decomposition products. Because of the presence of reduced oxomolybdates, platinum remained finely dispersed [25], as evidenced by the almost complete dissolution of mixture **II** in water with the formation of solution $\mathbf{II}_s$ containing Pt(0) and reduced heteropoly anions. Colloidal solution $\mathbf{II}_s$ produced platinum metal in air; this can be due to the reoxidation of heteropoly anions. On keeping a mixture of compounds **II** in air in the presence of oxygen and water vapor, the structure of heteropoly anions is readily regenerated with the formation of mixed-valence (Pt(II)/Pt(0) and Mo(VI)/Mo(V)) association species **III**, in which platinum particles are adsorbed on the surface of the HPA.

The catalytic properties of $(Pt_n^{II}Cl_mO_xH_y) \cdot (H_3PMo_{12}O_{40})$ ($\mathbf{I}_{solid}$) were studied after supporting the association species onto SiO_2 at $n = 0.66$ with 1.4% Pt and 20% $H_3PMo_{12}O_{40}$ ($\mathbf{I}_{solid}/SiO_2$).

The TPR with hydrogen allowed us to obtain data on the redox conversions of the HPA and platinum in supported $\mathbf{I}_{solid}$. In the absence of platinum, the 20% $H_3PMo_{12}O_{40}/SiO_2$ sample was reduced at a high temperature (Fig. 7a, curve *1*), and the absorption of H_2 in the range 400–600°C was ~10 mol per mole of the HPA. The reduction of the HPA in $\mathbf{I}_{solid}$ is catalyzed by platinum. The reduction of the 1.4% Pt · 20%$H_3PMo_{12}O_{40}/SiO_2$ sample occurred in the temperature range 100–250°C (Fig. 7a, curve *2*), and it can be approximated by two peaks with maximums at 130 and ~190°C (Fig. 7b). The amount of absorbed H_2 was 2.3×10^{-4} (peak I) and 5.5×10^{-4} mol (peak II) per gram of $\mathbf{I}_{solid}/SiO_2$. This corresponds to 2 and 5 mol of H_2, respectively, per mole of $Pt_{0.66} \cdot H_3PMo_{12}O_{40}$. It is believed that the reduced HPA $H_7PMo_8^{VI}Mo_4^{V}O_{40}$ is formed at the first step of the reaction of $\mathbf{I}_{solid}$ with H_2. At the second, more complicated step, Pt(0) (likely with adsorbed H_2) is formed, and a deeper reduction of the HPA occurs, probably, with the degradation of the Keggin structure [16]. In a replica cycle (performed after reaching a reduction temperature of 360°C, storing the sample in air, and treating it with oxygen at 300°C for 30 min), the absorption of H_2 in the temperature range 50–250°C was ~60% of the initial value (Fig. 7a, curve *3*). This can be due to the partial decomposition of the association species on the surface of SiO_2.

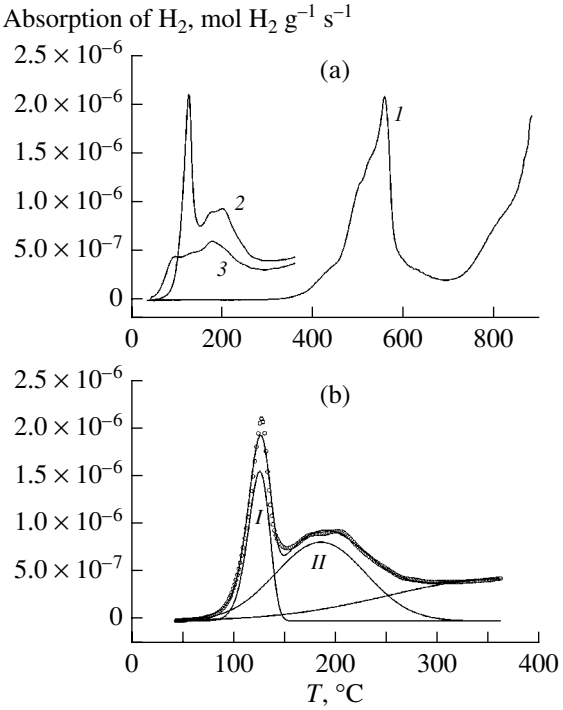

Fig. 7. (a) TPR curves of the samples of (*1*) 20% $H_3PMo_{12}O_{40}/SiO_2$ and (*2*, *3*) 1.4% Pt · 20% $H_3PMo_{12}O_{40}/SiO_2$: (*1*, *2*) first and (*3*) second TPR cycles; (b) approximation of curve *2* in Fig. 7a.

We monitored the states of platinum and heteropoly anions in $\mathbf{I}_{solid}/SiO_2$ using XPS. In the initial 1.4% Pt · 20%$H_3PMo_{12}O_{40}/SiO_2$ sample, the Pt4$f_{7/2}$ and Mo3$d_{5/2}$ binding energies were equal to 72.8 and 232.3 eV, respectively. The SiO_2-supported sample reduced with hydrogen (200°C; 1.5 h) contained molybdenum, probably, as a constituent of the deeply reduced HPA and products of its conversion (Mo3*d* doublets at 231.9 and 230.3 eV) and platinum metal (Pt4*f* doublet at 71.1 eV) [26] immediately after exposure to air (Figs. 8a, 8c). Moreover, a portion of platinum (~20%) occurred in a state with a binding energy of 72.8 eV. We attributed this binding energy to the association species of Pt(II) with the HPA. After keeping the sample in air for a day (Figs. 8b, 8d), the HPA was found reoxidized (Mo3*d* doublet at 232.4 eV, as in starting $\mathbf{I}_{solid}/SiO_2$). Platinum remained as a metal (Pt4*f* doublet at 71.3 eV); in addition, Pt(II) bound to the HPA (Pt4*f* doublet at 73.2 eV) was present.

The high-resolution transmission electron microscopic images of the supported association species $(Pt_n^{II}Cl_mO_xH_y) \cdot (H_3PMo_{12}O_{40})$ exhibited an insular component distribution over the SiO_2 surface both in the initial 1.4%Pt · 20%$H_3PMo_{12}O_{40}/SiO_2$ sample and

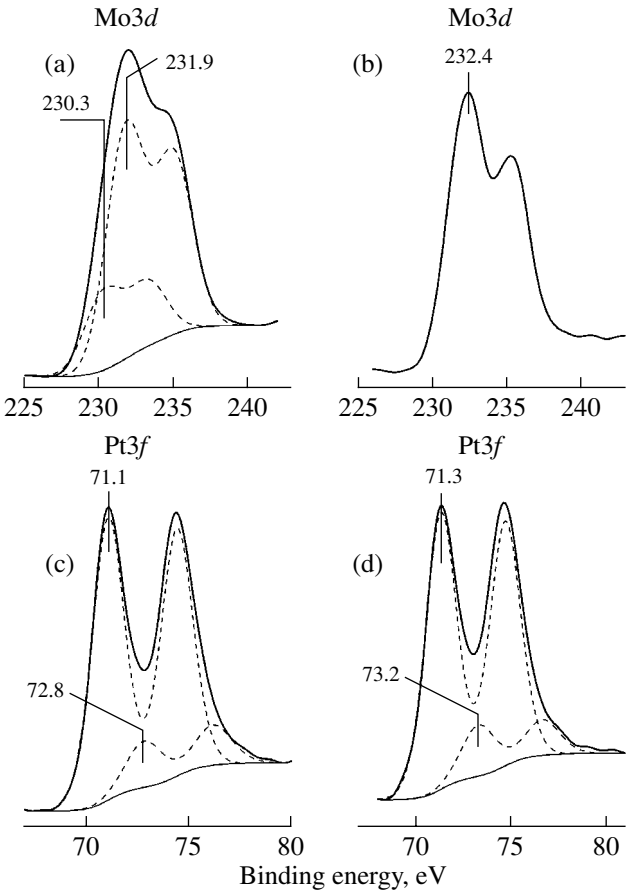

Fig. 8. XPS spectra of the sample of 1.4%Pt · 20%$H_3PMo_{12}O_{40}/SiO_2$: (a, c) measured immediately after reduction with hydrogen (200°C; 1.5 h) and (b, d) after keeping the reduced sample in air for a day.

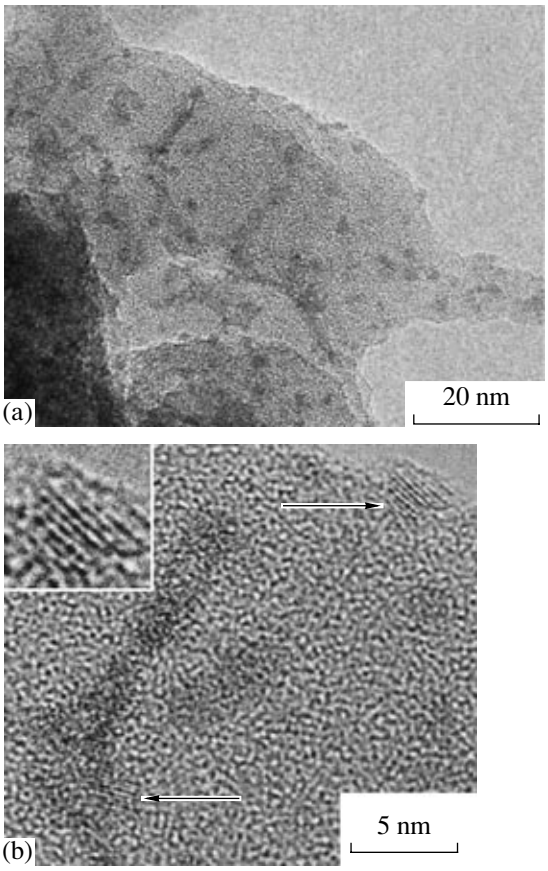

Fig. 9. Micrographs of the sample of 1.4%Pt · 20%$H_3PMo_{12}O_{40}/SiO_2$ (a day after reduction): (a) distribution of the supported component over the silica gel surface and (b) platinum metal as a constituent of islands; arrows indicate Pt particles with d_{111} = 0.227 nm.

after its reduction with hydrogen (1.5 h at 200°C) followed by keeping in air for a day (Fig. 9a). However, the structures of islands were different. The micrograph of the sample subjected to redox treatment (Fig. 9b) exhibited platinum metal particles of size ~2 nm with the Pt(111) lattice parameter 0.227 nm. The particles adjoined the supported component or occurred separately on the surface of silica gel.

The supported association species $(Pt_n^{II}Cl_mO_xH_y)\cdot(H_3PMo_{12}O_{40})$ on a 1.4%Pt · 20%$H_3PMo_{12}O_{40}/SiO_2$ basis was tested in benzene oxidation with an O_2–H_2 mixture. The sample without prereduction exhibited low activity in the formation of phenol (Fig. 10, curve *1*). Moreover, about 50% of the oxidized benzene was converted to CO_2. The reduction of the catalyst at the catalytic reaction temperature (T = 180°C; H_2–N_2 mixture, 10–85 ml/min; 1 h) increased the yield of phenol (Fig. 10, curve *2*). The sample pretreated with H_2 (200°C; 1.5 h) and kept in air for a day exhibited the highest activity in phenol formation (Fig. 10, curve *3*) (~10 mol of phenol per mole of Pt in an hour) and a lower CO_2 selectivity (33% of the oxidized benzene was converted to CO_2).

The increase of catalytic activity in the formation of phenol after sample reduction can be explained only by the presence of platinum metal in the test sample. However, platinum metal in the absence of the HPA was inactive in the selective oxidation of hydrocarbons. The oxidized forms of Pt(II) association species with the HPA, such as $\mathbf{I}_{solid}$, are almost inactive in the oxidation of benzene with an O_2–H_2 mixture. The synergism of these two constituents of the catalytic system consists in that platinum metal accelerates the hydrogen reduction of the association species of Pt(II) and the HPA with the formation of the mixed-valence compounds $(Pt_q^0Pt_{n-q}^{II}Cl_mO_xH_y)\cdot(H_{3+p}PMo_{12-p}^{VI}Mo_p^{V}O_{40})$. These compounds were prepared and characterized using spectroscopic techniques in the absence of SiO_2, and they were retained upon supporting onto SiO_2. Association species containing reduced platinum and HPA participate in the reductive activation of oxygen with

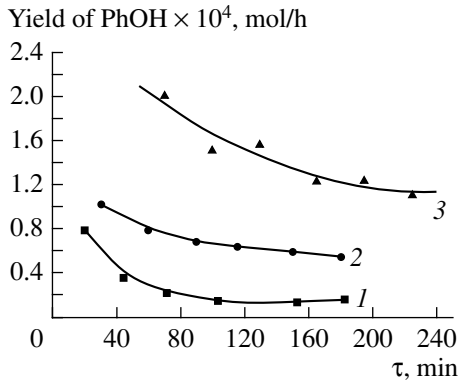

Fig. 10. Yield of phenol in the oxidation of benzene in the presence of 0.3 g of 1.4%Pt · 20%$H_3PMo_{12}O_{40}/SiO_2$: (*1*) initial, (*2*) after passing an H_2–N_2 mixture (10–85 ml/min; 180°C; 1 h), and (*3*) after reduction with H_2 (200°C) and keeping in air for a day. Conditions: 180°C; H_2, O_2, C_6H_6, and N_2 gas flow rates of 10, 5, 8, and 85 ml/min, respectively.

the formation of peroxide or radical oxygen species, which oxidize a substrate both in the liquid-phase systems studied previously [5] and in the gas-phase oxidation of benzene [6, 7].

CONCLUSIONS

Previously [6, 7], we found that a catalyst prepared by supporting molybdophosphoric HPA and H_2PtCl_6 onto SiO_2 (after pretreatment, calcination, and reduction stages and on keeping in air) exhibited high activity in benzene oxidation with the use of an O_2–H_2 mixture. In this work, we isolated and characterized the association species of Pt(II) and Pt(0) with the HPA formed at these stages. In these association species, both platinum and molybdenum ions are readily reduced with hydrogen and oxidized with oxygen with the retention of the interaction between platinum particles and the HPA. The same redox transformations also occurred after supporting the resulting association species $(Pt_n^{II}Cl_mO_xH_y) \cdot (H_3PMo_{12}O_{40})$ onto SiO_2. However, the reduction with hydrogen resulted in the partial degradation of the supported association species with the formation of finely dispersed platinum metal, which is not reoxidized with oxygen. The Pt–HPA association species supported on SiO_2 together with platinum metal exhibited catalytic activity in the reaction of benzene oxidation with an O_2–H_2 mixture. On this basis, they can be considered as two active catalyst components. Platinum metal activates hydrogen for the reduction of Pt(II) and Mo(VI) ions in the association species $(Pt_q^0Pt_{n-q}^{II}Cl_mO_xH_y) \cdot (H_{3+p}PMo_{12-p}^{VI}Mo_p^{V}O_{40})$, which, in turn, participates in the formation of active oxygen species.

ACKNOWLEDGMENTS

We are grateful to E.M. Moroz for helpful discussions of this work.

This study was supported by the Russian Foundation for Basic Research (project no. 03-03-32787) and the Council of the President of the Russian Federation (grant no. NSh-2287.2003.3).

REFERENCES

1. Kuznetsova, N.I., Detusheva, L.G., Kuznetsova, L.I., Fedotov, M.A., and Likholobov, V.A., *J. Mol. Catal. A: Chem.*, 1996, vol. 114, nos. 1–3, p. 131.
2. Kuznetsova, N.I., Kuznetsova, L.I., Detusheva, L.G., Likholobov, V.A., Fedotov, M.A., Koscheev, S.V., and Burgina, E.B., *Stud. Surf. Sci. Catal.*, 1997, vol. 110, p. 1203.
3. Kirillova, N.V., Kuznetsova, N.I., Kuznetsova, L.I., and Likholobov, V.A., *Izv. Akad. Nauk, Ser. Khim.*, 2002, no. 6, p. 894.
4. Kuznetsova, N.I., Kirillova, N.V., Kuznetsova, L.I., and Likholobov, V.A., *J. Molec. Catal. A: Chem.*, 2003, vols. 204–205, p. 591.
5. Kirillova, N.V., Kuznetsova, N.I., Kuznetsova, L.I., Zaikovskii, V.I., Koscheev S.V., and Likholobov V.A, *Catal. Lett.*, 2002, vol. 84, nos. 3–4, p. 163.
6. Kuznetsova, N.I., Kuznetsova, L.I., and Likholobov, V.A., *Katal. Prom–sti*, 2003, no. 4, p. 17.
7. Kuznetsova, N.I., Kuznetsova, L.I., Likholobov, V.A., and Pez, G.P., *Catal. Today*, 2005, vol. 99, p. 193.
8. Finke, R.G., in *Polyoxometalate Chemistry: From Topology via Self-Assembly to Applications*, Pope, M.T. and Müller, A., Eds., Dordrecht: Kluwer, 2001, p. 363.
9. Pavlova, S.N., Maksimovskaya, R.I., and Kuznetsova, L.I., *Kinet. Katal.*, 1991, vol. 32, no. 2, p. 410.
10. Moulder, J.F., Stickle, W.F., Sobol, P.E., and Bomben, K.D., *Handbook of X Ray Photoelectron Spectroscopy*, Eden Prairie, Minnesota, USA: Perkin-Elmer, 1992.
11. *Practical Surface Analysis by Auger and X-ray Photoelectron Spectroscopy*, Briggs, D. and Seah, M., Eds., Chichester: Wiley, 1983. Translated under the title: *Analiz poverkhnosti metodami Ozhe- i rentgenovskoi photoelektronnoi spektroskopii*, Moscow: Mir, 1987, p. 497.
12. Klementev, K.V., *Nucl. Instr. Meth. Phys. Res. A*, 2000, vol. 448, p. 299.
13. Gurman, S.J., Binsted, N., and Ross, I., *J. Phys. Chem.*, 1986, vol. 19, p. 1845.
14. Maksimovskaya, R.I. and Bondareva, V.M., *Zh. Neorg. Khim.*, 1994, vol. 39, no. 8, p. 1298.
15. Bondareva, V.M., Andrushkevich, T.V., Maksimovskaya, R.I., Plyasova, L.M., Litvak, G.S., and Burgina, E.B., *Kinet. Katal.*, 1997, vol. 38, no. 1, p. 122 [*Kinet. Catal.* (Engl. Transl.), vol. 38, no. 1, p. 106].
16. Mizuno, N., Katamura, K., Yoneda, Y., and Misono, M., *J. Catal.,* 1983, vol. 83, p. 384.
17. Maksimovskaya, R.I., Kuznetsova, L.I., and Matveev, K.I., *Koord. Khim.*, 1977, vol. 3, no. 5, p. 685.
18. Robin, M.B. and Day, P., *Adv. Inorg. Chem. Radiochem.*, 1967, vol. 10, p. 247.

19. Maksimov, G.M., Zaikovskii, V.I., Matveev, K.I., and Likholobov, V.A., *Kinet. Katal.*, 2000, vol. 41, no. 6, p. 925 [*Kinet. Catal.* (Engl. Transl.), vol. 41, no. 6, p. 844].

20. Kuznetsova, L.I., Maksimov, G.M., and Likholobov, V.A., *Kinet. Katal.*, 1999, vol. 40, no. 5, p. 688 [*Kinet. Catal.* (Engl. Transl.), vol. 40, no. 5, p. 622].

21. Prados, R.A. and Pope, M.T., *Inorg. Chem.*, 1976, vol. 15, no. 10, p. 2547.

22. Dorokhova, E.N. and Kazanskii, L.P., *Dokl. Akad. Nauk SSSR*, 1976, vol. 229, no. 3, p. 622.

23. Potapova, I.V., Kazanskii, L.P., and Spitsyn, V.I., in *Issledovanie svoistv i primenenie geteropolikislot v katalize* (Heteropoly Acids: Properties and Catalytic Applications), Yurchenko, E.N., Ed., Novosibirsk: Inst. Kataliza, 1978, p. 135.

24. Simonov, P.A., Troitskii, S.Yu., and Likholobov, V.A., *Kinet. Katal.*, 2000, vol. 41, no. 2, p. 281 [*Kinet. Catal.* (Engl. Transl.), vol. 41, no. 2, p. 255].

25. Ryndin, Yu.A., Kuznetsov, B.N., Moroz, E.M., Tripol'skii, A.A., and Ermakov, Yu.I., *Kinet. Katal.*, 1977, vol. 18, no. 6, p. 1536.

26. Ermakov, Yu.I., Ioffe, M.S., Ryndin, Yu.A., and Kuznetsov, B.N., *Kinet. Katal.*, 1975, vol. 16, no. 3, p. 807.